

# Electromagnetic equivalent model for phase conjugate mirror based on the utilization of left-handed material

Guoan Zheng<sup>1</sup>, Lixin Ran<sup>3</sup>, and Changhui Yang<sup>1,2</sup>

<sup>1</sup>Department of Electrical Engineering, California Institute of Technology, Pasadena, California 91125

<sup>2</sup>Department of Bioengineering, California Institute of Technology, Pasadena, California 91125

<sup>3</sup>Electromagnetics Academy at Zhejiang University, Zhejiang University, Hangzhou 310058, China  
[gazheng@caltech.edu](mailto:gazheng@caltech.edu)

**Abstract:** An electromagnetic equivalent model for the phase conjugate mirror (PCM) is proposed in this paper. The model is based on the unique property of the isotropic left-handed material (LHM) - the ability of LHM to reverse the phase factors of propagative waves. We show that a PCM interface can be substituted with a LHM-RHM (right-handed material) interface and associated image sources and objects in the LHM. This equivalent model is fully equivalent in the treatment of propagative wave components. However, we note that the presence of evanescent wave components can lead to undesirably surface resonance at the LHM-RHM interface. This artefact can be kept well bounded by introducing a small refractive index mismatch between the LHM and RHM. We demonstrate the usefulness of this model by modelling several representative scenarios of light patterns interacting with a PCM. The simulations were performed by applying the equivalent model to a commercial finite element method (FEM) software. This equivalent model also points to the intriguing possibility of realizing some unique LHM based systems in the optical domain by substituting a PCM in place of a LHM-RHM interface.

©2007 Optical Society of America

OCIS codes: (260.2110) Electromagnetic theory; (190.5040) Phase conjugation.

## References and links

1. B. Ya. Zel'dovich, R. F. Pilipetskii, and V. V. Shkunov, *Principles of Phase Conjugation* (Springer, Berlin, 1985).
2. R. A. Fisher, ed., *Optical Phase Conjugation* (Academic, New York, 1983).
3. R. Mittra and T. M. Habashy, "Theory of wave-front-distortion correction by phase conjugation," *J. Opt. Soc. Am. A* **1**, 1103-1109 (1984).
4. S. I. Bozhevolnyi, O. Keller, and I. I. Smolyaninov, "Scattered light enhancement near a phase conjugating mirror," *Opt. Commun.* **115**, 115-120 (1995).
5. P. Mathey, S. Odoulov, and D. Rytz, "Instability of single-frequency operation in semilinear photorefractive coherent oscillators," *Phys. Rev. Lett.* **89**, 053901 (2002).
6. J. de Rosny and M. Fink, "Overcoming the diffraction limit in wave physics using a time-reversal mirror and a novel acoustic sink," *Phys. Rev. Lett.* **89**, 124301 (2002).
7. B. E. Henty and D. D. Stancil, "Multipath-enabled super-resolution for rf and microwave communication using phase-conjugate arrays," *Phys. Rev. Lett.* **93**, 243904 (2004).
8. G. Lerosey, J. de Rosny, A. Tourin, M. Fink, "Focusing Beyond the Diffraction Limit with Far-Field Time Reversal," *Science* **315**, 1120-1122 (2007).
9. M. Cronin-Golomb, J. O. White, A. Yariv, B. Fischer, "Theory and applications of four-wave mixing in photorefractive media," *IEEE J. Quantum Electron.* **20**, 12-30 (1984).
10. A. A. Zozulya, and V. T. Tikhonchuk, "Investigation of stability of four-wave mixing in photorefractive media," *Phys. Lett. A* **135**, 447-452 (1989).
11. P. C. Yeh, *Introduction to Photorefractive Nonlinear Optics* (Wiley, New York, 1993).
12. Z. Yaqoob, D. Psaltis, M. S. Feld, and C. Yang, "Optical phase conjugation for turbidity suppression in biological samples," submitted to *Nature Photonics*.
13. D. R. Smith and N. Kroll, "Negative Refractive Index in Left-Handed Materials," *Phys. Rev. Lett.* **84**, 4184 (2000).
14. J. B. Pendry, "Negative Refraction Makes a Perfect Lens," *Phys. Rev. Lett.* **85**, 3966 (2000).

15. J. Pacheco, T. M. Grzegorzczak, B. I. Wu, Y. Zhang, and J. A. Kong, "Power Propagation in Homogeneous Isotropic Frequency-Dispersive Left-Handed Media," *Phys. Rev. Lett.* **89**, 257401 (2002).
16. M. Nieto-V. and E. Wolf, "Phase conjugation and symmetries with wave fields in free space containing evanescent components," *J. Opt. Soc. Am. A* **2**, 1429-1434 (1985).
17. J. A. Kong, *Electromagnetic Wave Theory*, (EMW Publishing, 2005) Chaps. 3, 5.
18. N. Engheta, "An idea for thin subwavelength cavity resonators using metamaterials with negative permittivity and permeability," *IEEE Antennas Wireless Propag. Lett.* **1**, 10-13 (2002).
19. Y. Li, L. Ran, H. Chen, J. Huangfu, X. Zhang, K. Chen, T. M. Grzegorzczak, and J. A. Kong, "Experimental realization of a one dimensional LHM-RHM Resonator," *IEEE Trans. Microwave Theory and Tech. special issue on Metamaterials* **53**, 1522-1526 (2005).
20. S. He, Y. Jin, Z. Ruan and J. Kuang, "On subwavelength and open resonators involving metamaterials of negative refraction index," *New J. Phys.* **7**, 210 (2005).
21. T. J. Cui, Q. Cheng, W. B. Lu, Q. Jiang and J. A. Kong, "Localization of electromagnetic energy using a left-handed-medium slab," *Phys. Rev. B* **71**, 045114 (2005).
22. COMSOL Multiphysics 3.3 (2007), *COMSOL INC.* (<http://www.comsol.com/>)

## 1. Introduction

Phase conjugation is an interesting wave phenomenon in which both the direction of propagation and the overall phase factor for each arbitrary plane wave are precisely reversed during reflection from a phase conjugate mirror (PCM) [1, 2]. A propagative wave reflected by the PCM will retrace its original path back to the source. Thus if one is mirrored by a PCM, he/she will see nothing but his/her own pupils, or to be more specific, he/she will see his/her left pupil with his/her left eye and he/she will see his/her right pupil with his/her right eye. The PCM has been used to compensate for optical signal distortions [3], to enhance near-field light components [4], and to construct some novel interferometers and resonators [1, 5]. Moreover, the field of phase conjugation has been extended into other areas, including RF and acoustic analogs of the optical phenomenon [6-8]. A typical method to construct an optical PCM is carried out by a four-wave mixing process where a refractive index grating induced by interference of two beams diffracts another beam to generate the phase conjugated beam [9-11].

Recently, our group demonstrated that phase conjugation can be used to suppress elastic optical scattering in biological tissues [12]. Due to the random nature of the scattering site arrangements in tissues and the high number of scattering involved, computational simulation models for the interaction between PCM and biological tissues are difficult to implement. Yet, accurate simulation models that are computationally efficient are very much desired in aiding us better understand this newly observed biophotonics phenomenon.

In this paper, we report on an electromagnetic equivalent model that allows for simulations of phase conjugation in a computationally efficient manner. This model, based on the substitution of the PCM interface with a left handed material (LHM) [13-15] and an appropriately altered duplicate of the space before the PCM interface, simplifies computations of propagative wave components' interactions with PCM. Briefly, this simplification can be appreciated through the following analogy. The electric field distribution of a point charge placed at a distance from a grounded conductive interface can be easily solved by replacing the interface by a virtual point charge with the opposite charge at the same distance behind the interface. In much the same way, the substitution of the PCM with an extended LHM and appropriate image-source is a relatively easier approach for performing simulations.

Due to LHM's unique properties, LHM has drawn much attention from the scientific communities. An LHM's permittivity and permeability are both negative, and thus it has a negative index of refraction. The unique electromagnetic (EM) properties exhibited by LHM obey Maxwell equations, and do not violate any known physical laws [13-15]. Of special interest to us is the LHM's ability to reverse the phase factor of propagative waves in much the same way as a PCM would.

This paper is structured as follows. In Section 2, we describe the electromagnetic equivalent model and illustrate its ability to simulate the interaction of propagative wave components with a PCM. In Section 3, we describe an approach for keeping simulations bounded by suppressing the effect of evanescent waves which can generate undesirably

surface resonance at the interface between RHM (right handed material) and LHM. In Section 4, we report on our simulation demonstrations that points to the feasibility of this model. In Section 5, we summarize our findings and discuss some of the possible applications.

## 2. The equivalent model for propagative wave components

We shall start with a simple scenario which is depicted in Fig. 1(a). For simplicity, we will limit our discussion to a unit gain PCM here and through out the rest of the paper – in other words, it fully reflects all incident waves and induces no loss at the PCM interface. The scenario depicts the scattering of light (black lines) from a uniform incident wave by a spherical scatterer ( $\epsilon_s, \mu_s$ ). The permittivity and permeability of the background medium are assumed to be  $\epsilon_0, \mu_0$ . The scattered wave impinges upon a PCM and generates a phase conjugate reflected component. This wave will retrace its path back to the scatterer; this is a key property of PCM. Mathematically, if the incident wave's electric component at the PCM interface is expressed as  $E_0(x, z)$  and the phase-conjugate reflected wave at the PCM interface can be expressed as  $E_0^*(x, z)$ . The total electric field at the interface must satisfy:

$$\text{Re}(E) = 2 \text{Re}(E_0), \text{Im}(E) = 0 \quad (1)$$

The zeroing of the imaginary component of the E-field at the interface is a unique property of the PCM.

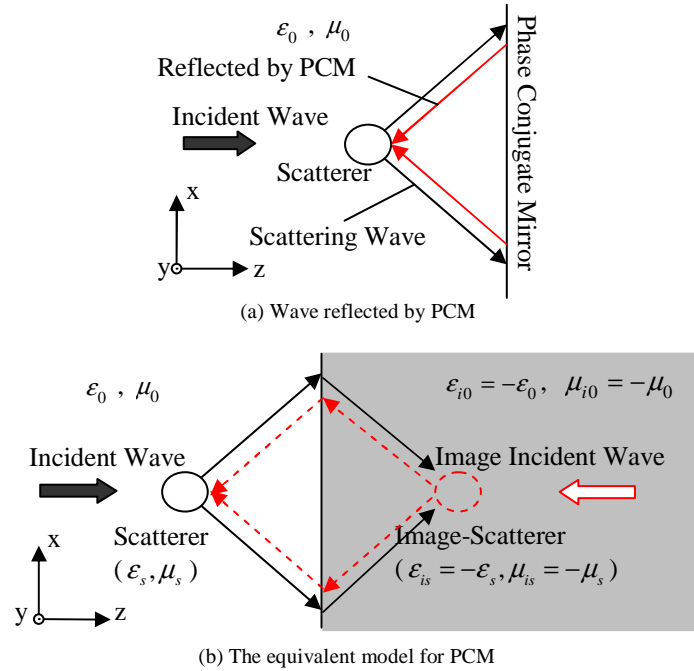


Fig. 1. (a). A scatterer is placed in front the PCM. (b). The proposed equivalent model for propagative wave components.

Next we consider the scenario where we replace the PCM with a half-space LHM (denoted as the grayed region) with  $\epsilon_{i0} = -\epsilon_0$  and  $\mu_{i0} = -\mu_0$ . As a consequence, the refractive index will also be similarly inverted ( $n_{i0} = -n_0$ ). We add an image scatterer ( $\epsilon_{is} = -\epsilon_s, \mu_{is} = -\mu_s$ ) and an image incident wave in the LHM symmetrically about the interface. Assuming that the electric-field at the surface generated by the incident wave and its

interaction with scatterers is given by  $E_1 \cdot e^{i\varphi}$ , the corresponding electric field generated by the image incident wave and its interaction with the scatterers should be  $E_1 \cdot e^{-i\varphi}$ . No reflection occurs at the interface since the match is perfect. The reversing phase factor in  $E_1 \cdot e^{-i\varphi}$  is due to the fact that when the image incident wave propagates towards the interface, the phase factor is negatively accumulated (the phase velocity and the group velocity are contra-directional inside an isotropic LHM). Thus the total field  $E$  at the surface satisfies

$$\text{Re}(E) = 2 \text{Re}(E_1 \cdot e^{i\varphi}), \text{Im}(E) = 0 \quad (2)$$

, which has the same form as in Eq. (1). As the field distributions at the boundary are the same and the original sources in the region of interest are preserved in both scenarios, both scenarios should lead to the same solution in the region of interest by the equivalent principle [17]. Therefore we can treat the configuration in Fig. 1(b) as an equivalent model for the configuration in Fig. 1(a), as long as we are only interested in the region to the left of the interface. The above discussion is only valid for the propagative wave components; we will discuss treatment of the evanescent wave components in the next section.

As any given propagative wave can be decomposed into a set of constitutive plane waves at the interface, and each plane waves can be treated at the PCM by this approach individually, this approach is generally applicable for all propagative waves.

### 3. The treatment of evanescent wave components

The discussion in the above section is strictly valid for situations where we only have propagative wave components incident on the PCM. However, in many cases, the scattered waves can also contain significant evanescent wave components. The treatment of evanescent wave in our model requires special attention.

Consider the scenario that an evanescent wave incident upon on the PCM. For the real PCM case, such wave will attenuate exponentially when it travels towards the PCM and the reflected evanescent wave will still attenuate exponentially as it travels back to the source [16]. Therefore, we can expect the reflection of evanescent wave from a PCM to lead to a bounded and well behaved solution. Incidentally, the continued decay of the evanescent wave upon reflection from a PCM is the reason phase conjugation can not be considered as a true 'time reversal' phenomenon [16]. While the propagative wave components are time direction symmetric under phase conjugation, the same cannot be said for the evanescent wave components.

The treatment of evanescent wave components in our equivalent model is nuanced. For the model, the presence of an evanescent wave will imply the existence of an image evanescent wave. When the two meets at the interface of RHM and LHM, they will experience an infinitely enhancement at the interface if the match of RHM and LHM is perfect. In other words, a perfectly matched LHM and RHM interface will infinitely amplify the evanescent wave components.

There are at least two approaches to keep the model bounded and usable in the context of managing this runaway resonance effect. The first approach is to apply the model in situations where there are strictly no evanescent components. This approach is somewhat constraining and limiting. The second approach is to introduce a small refractive index mismatch between LHM and RHM. This eliminates the undesirable presence of an infinitely large enhancement, and at the same time, allows the propagative wave components to behave almost exactly as they would in a perfectly matched LHM-RHM case.

To clarify this refractive index mismatch approach, consider a source that is placed in the RHM region at a distance  $L$  away from the interface of RHM and LHM. The image source is similarly placed in the LHM. For convenience, we shall normalize the amplitude of all waves, including both propagative and evanescent components to be one at the source. For a TE wave incident at the interface with the E-field polarized along the y-direction, the reflection and

transmission coefficient R and T can be calculated by [14] (the treatment of the image source can be done in the same manner)

$$R = \frac{k_z^i / \mu_0 - k_z^t / \mu_{i0}}{k_z^i / \mu_0 + k_z^t / \mu_{i0}} e^{ik_z^i L}, T = \frac{2k_z^i / \mu_0}{k_z^i / \mu_0 + k_z^t / \mu_{i0}} e^{ik_z^i L} \quad (3)$$

, where

$$k_z^i = \begin{cases} +\sqrt{\varepsilon_0 \mu_0 k_0^2 - k_x^2} & (\varepsilon_0 \mu_0 k_0^2 - k_x^2 > 0) \\ +i\sqrt{k_x^2 - \varepsilon_0 \mu_0 k_0^2} & (\varepsilon_0 \mu_0 k_0^2 - k_x^2 < 0) \end{cases} \quad (4a)$$

$$k_z^t = \begin{cases} -\sqrt{\varepsilon_{i0} \mu_{i0} k_0^2 - k_x^2} & (\varepsilon_{i0} \mu_{i0} k_0^2 - k_x^2 > 0) \\ +i\sqrt{k_x^2 - \varepsilon_{i0} \mu_{i0} k_0^2} & (\varepsilon_{i0} \mu_{i0} k_0^2 - k_x^2 < 0) \end{cases} \quad (4b)$$

In Eq. (3) and (4),  $k_0$  is the wave number in the vacuum;  $k_x$  is the transverse wave number;  $k_z^i$  is the z-direction incident wave number in the RHM, and  $k_z^t$  is the z-direction transmission wave number in the LHM, respectively. Notice that the real part of  $k_z^t$  is negative because the phase and group velocity are contra-directional in the LHM, that is when the energy of the propagative wave is traveling in the -z direction, the phase velocity will point in the +z direction. On the other hand, the imaginary part of  $k_z^t$  should be a positive value because of the causality: the wave in LHM must decay away exponentially from the interface, as demonstrated in Ref. [14]. The term  $e^{ik_z^i L}$  in Eq. (3) is due to the fact that we normalized the field to be 1 at the source, i.e., at the distance  $L$  from the interface.

In the case where the RHM and LHM are perfectly matched (i.e.  $\varepsilon_{i0} = -\varepsilon_0$ ,  $\mu_{i0} = -\mu_0$ ), the reflection and transmission coefficient will go to infinity for the evanescent wave, because  $k_z^i / \mu_0 + k_z^t / \mu_{i0}$  equals to 0 in Eq. (3) when  $\varepsilon_0 \mu_0 k_0^2 - k_x^2 < 0$ . This leads to the aforementioned difficulty.

This undesirable amplification of the evanescent wave can be effectively eliminated by introducing a small mismatch  $\delta$  between RHM and LHM, i.e.  $\varepsilon_{i0} = -\varepsilon_0 - \delta$ ,  $\mu_{i0} = -\mu_0 - \delta$  instead of  $\varepsilon_{i0} = -\varepsilon_0$ ,  $\mu_{i0} = -\mu_0$ .

As an illustration, the magnitude of the reflection and transmission coefficient R and T is plotted in Fig. 2 as a function of the transverse wave number  $k_x$ , with  $L = 5\lambda$  and different mismatch term  $\delta$ 's (we simply assume  $\varepsilon_0 = \mu_0 = 1$  in our calculation). One can see that the choice of  $\delta$  is a tradeoff between eliminating the surface resonance and retaining an accurate model of propagative wave components' behavior. If the  $\delta$  is closer to 0, the behavior of propagative wave component will remain very similar to the perfectly matched LHM-RHM case, while the surface resonance can not be effectively eliminated. If the  $\delta$  is larger, the surface resonance can be well eliminated but the propagative component may also decrease. As shown in Fig. 2, for the case of  $L = 5\lambda$ ,  $\delta = 0.001$  may be a good choice since the evanescent wave component with  $k_x > k_0$  is greatly eliminated, meanwhile the R and T for propagative wave (i.e.  $k_x < k_0$ ) are only slightly affected.

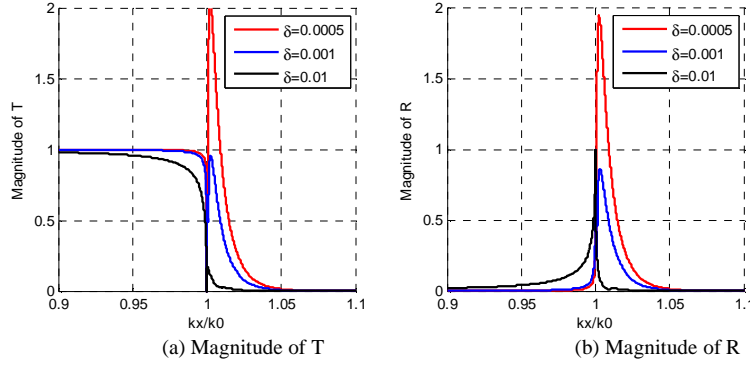


Fig. 2 The reflection and transmission coefficient as a function of  $k_x$  with  $L=5\lambda$ , and different mismatch term  $\delta$  s. (a) Magnitude of T, (b) Magnitude of R.  $k_x/k_0 < 1$ : propagative wave components,  $k_x/k_0 > 1$ : evanescent wave components.

In Fig. 3, we plot the case for  $L=10\lambda$ . As  $L$  is larger in this case, the strengths of the evanescent wave components are strongly attenuated prior to reaching the interface. We can see from the figure that even a small refractive index mismatch is able to bind the model to a well behaved regime in this case. This clearly illustrates the utility of the refractive index mismatch in dealing with evanescent wave components in simulations based on our equivalent model. The choice of the refractive index mismatch depends on the accuracy of the propagative wave simulation desired and the strengths of the evanescent wave components at the interface.

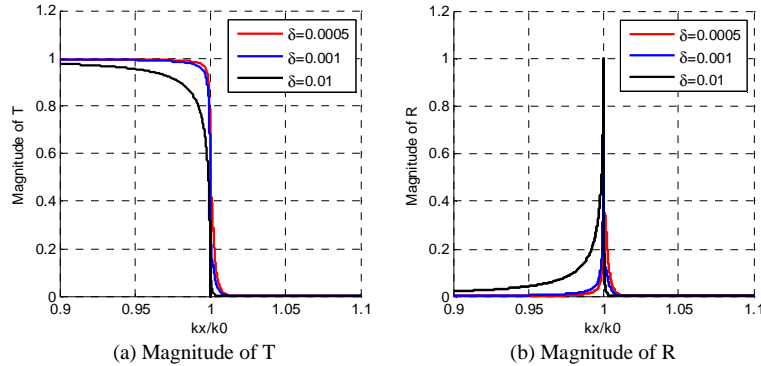


Fig. 3. The reflection and transmission coefficient as a function of  $k_x$  with  $L=10\lambda$ , and different mismatch term  $\delta$  s. (a) Magnitude of T, (b) Magnitude of R.  $k_x/k_0 < 1$ : propagative wave components,  $k_x/k_0 > 1$ : evanescent wave components.

#### 4. Simulations of different scenarios

In order to demonstrate the feasibility of our model for PCM, we performed a simulation study for three scenarios. The simulations are conducted by a commercial finite element method (FEM) simulation program, Comsol [22].

The first scenario was a point source radiation case - an electric dipole radiates energy at the position  $5\lambda$  in front of the PCM. We carried out a simulation of E-field intensity distribution for this scenario based on the proposed equivalent model, as shown in Fig. 4(a). The computational domain was  $20\lambda \times 40\lambda$  enclosed by perfect match layer (PML) as the absorption boundary. We introduced a small mismatch  $\delta=0.001$  for the LHM. As a

comparison, two other simulations were also conducted. One was the case where we replaced the PCM with a conventional mirror (perfect electric boundary), the other was the case where the interface was replaced by a PML boundary, as shown in Fig. 4(b) and Fig. 4(c) respectively. The computational domain was  $10\lambda \times 40\lambda$  for these two control simulations. The fringes highlighted in Fig. 4(a) were due to the interference between the incident wave and the reflected phase-conjugate wave. One can even find the interference fringes near the dipole-source as pointed out by white arrow in Fig. 4(a). Such near-source circle-like interference fringe is a unique property for PCM, because it indicates that the reflected phase-conjugate wave retraces its original path back to the source and interferes with the incident wave. For the case of conventional mirror in Fig. 4(b), the interference fringes near the reflecting plane were line-like, parallel to the reflecting plane. For the last case shown in Fig. 4(c), no fringe can be found since there was no possibility of waves interfering with each other.

The second scenario was a diffraction case - a phase grating was placed at the position  $5\lambda$  in front of the PCM and a point source illuminated the grating (Fig. 5(a)). We introduced a small mismatch  $\delta = 0.001$  for the LHM in the simulation. The width and period of the grating were  $\lambda/8$  and  $\lambda$  respectively, as shown in Fig. 5(a). The permittivity and permeability of the grating were set at 4 in the simulation. Two point sources were used to generate the incident and image incident waves. These two point sources are placed  $9\lambda$  away from the interface. As shown in Figs. 5(b) and 5(c), the case with conventional mirror and the case with a PML boundary are also shown for comparison. From Fig. 5, one can see that the wave radiated by the point source was diffracted by the phase grating and the interference fringe can be found in the diffracted beam, as indicated by a white arrow in Fig. 5(a). Such fringe indicated strong interference between the diffracted wave and the phase conjugate reflected wave.

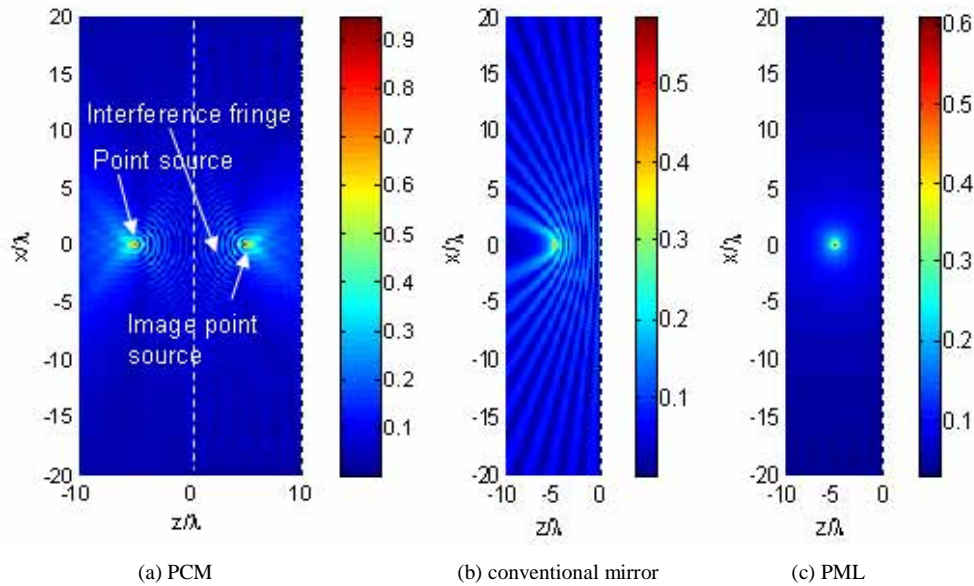


Fig. 4. The E-field intensity distribution for the point source radiation scenario. (a) equivalent model of PCM, (b) conventional mirror and (c) perfect match layer boundary.



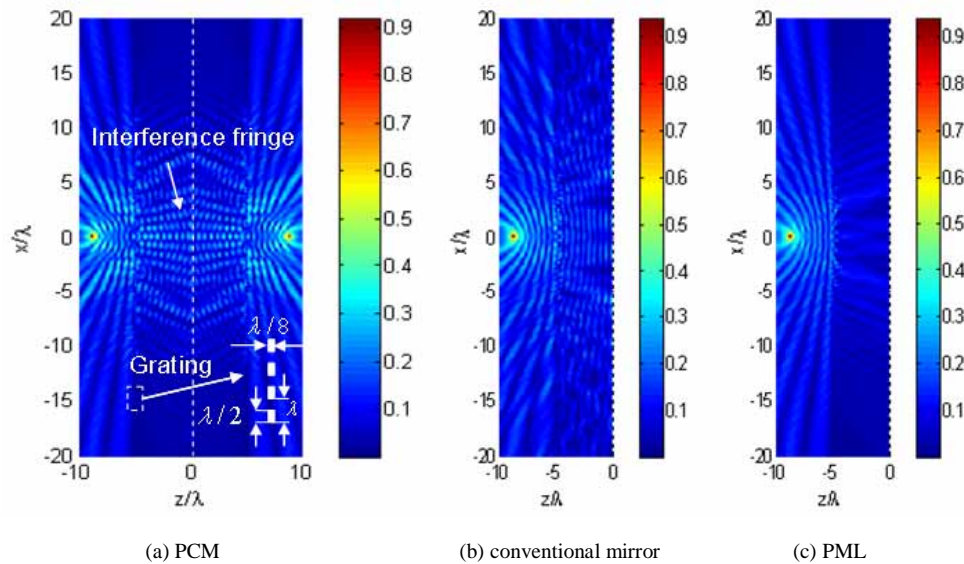


Fig. 5. The E-field intensity distribution for the diffraction scenario. (a) equivalent model of PCM, (b) conventional mirror and (c) perfect match layer boundary.

The third second scenario was a scattering case - a sphere scatterer with  $\epsilon_s = \mu_s = 4$  was placed at the position  $5\lambda$  in front of the PCM and a port source illuminated the scatterer [Fig. 6(a)]. We introduced a small mismatch  $\delta = 0.001$  for the LHM in the simulation. Two waveguide ports were used as the sources to generate the incident and image incident waves. These two ports were both  $1\lambda$  wide and placed  $10\lambda$  away from the interface. As shown in Figs. 6(b) and 6(c), the case with conventional mirror and the case with a PML boundary are also shown for comparison. From Fig. 6, we can see interference fringes between the scatterer and the PCM. The fringes once again indicate strong interference between scattering and phase-conjugate reflected wave.

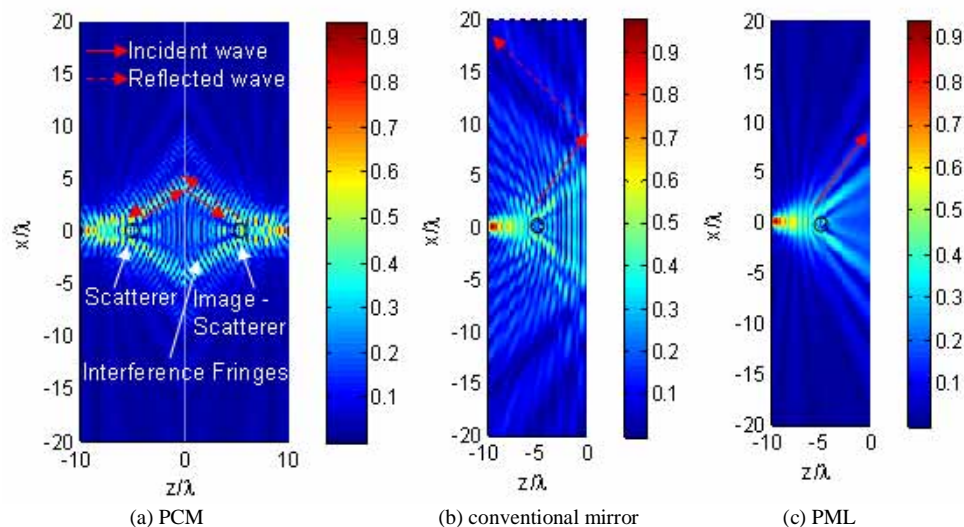


Fig. 6. The E-field intensity distribution for the scattering scenario. (a) equivalent model of PCM, (b) conventional mirror and (c) perfect match layer boundary.



## 5. Conclusion

In this paper, we report on an electromagnetic equivalent model that allows for the simulation of phase conjugation in a computationally efficient manner. The equivalent model is based on the unique property of left-handed material - the ability of LHM to reverse the phase factor of the propagative wave. Using this model, we can more easily simulate the reflection of any propagative light field from a PCM. However, we note that this model is not designed to accommodate evanescent wave components at the LHM-RHM interface – undesirably large enhancement of evanescent wave can occur at the interface. We show that a small refractive index mismatch between the two materials can be used to keep this resonance bounded. On the other hand, this fix does lead to some small errors in the computation of the propagative wave components. The choice of the mismatch can be optimized on a case by case basis.

Using the proposed model, a simulation study on PCM is carried out based on a conventional electromagnetic computational method for the first time. For the point source radiation scenario, near-source circle-like interference fringes are found and they converge to the point of origin-source. This fringe pattern is a unique feature of reflections from PCM as it derives from the interference of the original and optical phase conjugate waves. Similar fringes can also be found in our simulation case studies of a diffraction grating and a scatterer. This study demonstrates the usefulness of the proposed model for adapting conventional electromagnetic simulation methods and commercial electromagnetic wave simulation software for studying interactions with PCM.

From another point of view, this equivalent model points to some similarities between PCM and a LHM-RHM interface [18-21]. Intriguingly, this suggests it may be possible to substitute a LHM-RHM interface with a PCM as a means to more easily realize some of the unique LHM based systems that have been conceived. For example, Engheta [18] proposed to use a layer of LHM and a layer of the conventional right-handed material to construct a size-independent resonator – a resonator whose size can be much smaller than the working wavelength. Such size-independent effect of RHM-LHM resonator had recently been experimentally verified [19]. Based on the proposed equivalent model, such size-independent resonator can also be realized by a layer of conventional right-handed material and a PCM. The use of a PCM in place of a LHM simplifies implementation in the optical regime.

Finally, we will like to note that there exist a range of experimental scenarios in which the PCM may have a non-unit gain factor. This means that the E-field of the reflected wave equals to  $CE_0^*(x, z)$ , where C is the reflection efficiency coefficient of PCM. At the moment, it is unclear how a low or high efficiency PCM can be best modeled. This subject is important and deserves more future study and analysis.

## Acknowledgments

This work was supported by NSF career award BES-0547657.